

UNCERTAINTY ASSESSMENT OF NEAR-EARTH ASTEROID SIZE MEASUREMENTS FROM RADAR IMAGES. E. A. Whittaker^{1,2}, P. A. Taylor¹, E. G. Rivera-Valentín¹; ¹Lunar and Planetary Institute, Universities Space Research Association, Houston, TX 77058, ²Department of Astronomy, University of Maryland, College Park, MD 20742 (ewhittak@terpmail.umd.edu).

Introduction: Planetary defense strategies rely on the detection and characterization of near-Earth asteroids (NEAs). Of importance are robust constraints on the sizes of asteroids that are potentially hazardous to Earth. Wide-field infrared surveys, such as NEOWISE, use the Near-Earth Asteroid Thermal Model [1] to infer sizes for many asteroids; however, the method is indirect and assumes a spherical shape. Ground-based planetary radars, such as the Arecibo Observatory, can provide precise and direct size measurements; however, confident constraints on the three-dimensional shape requires time intensive inverse modeling using data over different viewing geometries and rotational phase coverage. On the other hand, single delay-Doppler images (e.g., Fig. 1) can quickly provide bounds on an object's size by direct measurement of the echo depth along the delay axis. The uncertainty of such a measurement, though, depends on many variables, including resolution, signal strength, pole direction, and shape.

Here we test the uncertainty of measuring an NEA's size directly from a delay-Doppler image. We focus on the simple case of spheroidal objects and assess the uncertainty of size measurements as a function of signal strength using both manual and automated techniques.

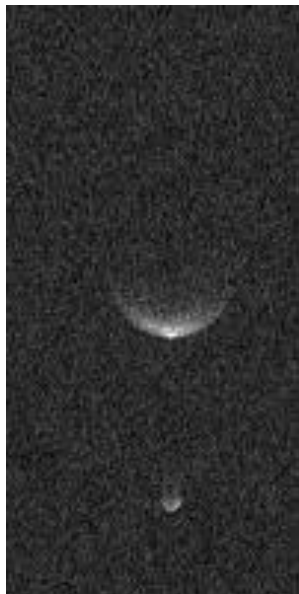


Figure 1: Delay-Doppler image of 66391 Moshup (1999 KW4) and its moon, taken on May 30, 2019 using the Arecibo Observatory. This image is 30 m/pixel, with the horizontal axis indicating Doppler shift and the vertical axis indicating time delay/range.

Methods: In our study, we used the recent observing campaign of NEA 66391 Moshup (1999 KW4, hereafter KW4) as a test case. KW4 is a binary system (see Fig. 1) with a well-

defined shape model [2]; it is an oblate spheroid with dimensions of $1.532 \times 1.495 \times 1.345$ km and an equivalent spherical diameter of 1.317 km [2]. We estimated the size via visual inspection, which involves estimation by eye of the echo depth in delay-Doppler images from the leading edge of the echo to the furthest visible extent, and three statistical techniques that analyzed the echo power mathematically.

Visual Inspection. The extent of the echo was assessed by visually identifying the leading edge, which is well defined by its signal strength, and the trailing edge of the echo as the last pixel row where the outer “wing” portions of the signal were still visually distinguishable from the background noise. We used this technique for synthetic radar images from a noiseless spherical model as well as for radar images of KW4.

Linear Fit. Delay-Doppler images were reduced to relative echo power spectrums along the delay axis (e.g., Figure 2). The points preceding and following the maximum signal that had an echo power greater than zero were referred to as the first and last points respectively. We used a linear least-squares fit to the data between the last and maximum points to identify the y-intercept, which corresponds to the maximum extent of the echo. The difference between the first point and the y-intercept was our estimate of the radius.

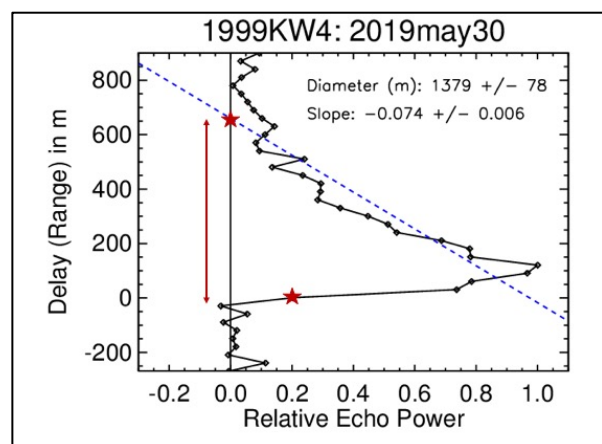


Figure 2: Plot of range (m) vs. relative echo power of KW4. The linear fit to the data is the blue dotted line. The red arrow between the two red stars estimates the radius.

Scattering Law Fit. The shape of the echo power with respect to delay is a function of the radar scattering properties of the target body. Thus, here we consider a cosine scattering law of the form

$$\sigma_0(\theta) \sim \left(\frac{n+2}{2}\right) \cos^n(\theta)$$

where n is typically ~ 2 , θ is the incidence angle, and $\sigma_0(\theta)$ is proportional to the echo power [3]. The scattering law can be rewritten as

$$\text{echo power} \sim \left(1 - \frac{\text{range}}{R}\right)^n$$

where R is the best fit radius and n is the power of the cosine law. Data used in this fit were constrained to between $25^\circ \leq \theta \leq 80^\circ$ as this range for KW4 was estimated to have scattering properties most similar to this simple scattering law. The polar and the equatorial regions of KW4 may have scattering properties that deviate from a spherical model due to the asteroid's top-like shape. The best fit radius for this model was found to be where χ^2 was minimized for a range of n and R values. R and n tended to be well constrained for spherical models, but were poorly constrained for noisy images and non-spherical models, resulting in unreasonably large values of R and n .

Noise Statistics Method. To obtain an estimate of the radius without making assumptions about the shape of the echo-power function, we used noise statistics to identify the extent of the asteroid's signal. We created an algorithm which calculates the mean value of a set of data points within the echo power plot and compares this to the standard deviation of the portion of the plot most closely representing statistical noise. The initial set of points was chosen from beyond the visible echo and shifted incrementally closer to the visible echo, taking the mean value before each shift. When the mean of the tested set exceeded 1.5σ , we took the signal to end at the midpoint of the final set.

Results: Using visual inspection, the radius of KW4 in real images was underestimated by 45.2% and the radius of a noiseless spherical model was even underestimated by 20.4%. Table 1 shows the percent error for the three studied statistical techniques. The percent error values were calculated by averaging over the total number of images, where there are 5 images of the noiseless spherical model, 3 actual radar images of KW4, and 106 synthetic noiseless images from the *Shape* model of KW4. The uncertainty for each value was taken to be the standard deviation in the average percent error. Percent error calculations were based on an equatorial radius of 0.75 km for the spherical model, an assumed radius of 0.75 km for KW4, and the leading edge to center-of-mass radius for each image within the KW4 shape model.

Error in Radius (%)			
	Spherical Model	1999 KW4	1999 KW4 Shape Model
Linear	17.2 ± 0.3	9.6 ± 4.7	5.2 ± 0.5
Scattering	1.1 ± 0.2	67 ± 30	78.6 ± 5.7
Statistical	5.3 ± 0.4	16.7 ± 6.8	14.3 ± 1.4

Table 1: Percent error measurements for methods of radius measurement and data types. Errors are represented as a percentage, with blue where the majority of errors are underestimations and yellow where the majority of errors are overestimations.

Conclusions: Compared to the statistical techniques, the significant underestimations in radius obtained using the visual inspection technique demonstrate the inability to accurately assess NEA radii by eye. On the other hand, the scattering law fit required that a radar image have an uncharacteristically high signal-to-noise ratio (SNR) to obtain an accurate radius estimate. The noise statistics technique was the most robust technique for radar images with a low SNR, but its accuracy relies on the radar image having a high enough resolution in delay/range that there are enough data points to avoid using unreliable small number statistics. The linear fitting technique was the most reliable technique as its average percent error never exceeded 18%, and the error tended toward underestimation, allowing for a global corrective factor that could be applied in many cases. Future investigation into the linear fitting and noise statistics methods should be done to improve the accuracy of NEA radii measurement.

References: [1] Mainzer A. K. et al. (2015) *Asteroids IV*, 89-106. [2] Ostro S. J. (2006) *Science* 314, 1276-1280. [3] Ostro S. J. (2007) *Encyclopedia of the Solar System (Second Edition)*, 3.6.

Acknowledgements: This research resulted from the LPI Summer Internship program. LPI is operated by Universities Space Research Association under a cooperative agreement with the Science Mission Directorate of NASA. The work was also supported by NASA through the NEOO program under Grant No. NNX13AQ46G. The Arecibo Observatory is a facility of the NSF managed under cooperative agreement by UCF in alliance with Yang Enterprises, Inc., and Ana G. Méndez University.